Transonic Flow in Nozzles Using the Method of Integral Relations

S. G. LIDDLE*
General Motors Research Laboratories, Warren, Michigan

AND

R. D. ARCHER†
University of New South Wales, Sydney, Australia

The method of integral relations has been adapted to solve the inviscid compressible flowfield equations for a perfect gas in axisymmetric nozzles of arbitrary shape, and in particular for conical nozzles commonly used in rockets. Experiments to measure both wall and centerline pressures on conical nozzles were performed with cold air in order to test the method. Ahead of the wall curvature discontinuity in the diverging supersonic region, agreement of first-order theory with experimental wall pressures is good for throat radii of curvature greater than two times the throat radius, but higher order theory is required otherwise. Such higher order solutions, however, require iterations on additional unknown initial conditions and a corresponding increase in computer time and difficulty in numerical procedures. Conditions leading to formation of shocks as observed in the experiments are predicted by the method. In the absence of wall curvature discontinuity and of shock waves the method can be used to provide the complete flowfield.

Nomenclature‡

a,b = numerical coefficients, see Eqs. (17) and (18)
f = axial velocity w, or mass flux ρw, see Eq. (17)
F = flow rate, Eqs. (21, A7, and B10)
N = number of strips (Fig. 1)
n = coordinate conversion factor (zero for Cartesian, one for cylindrical)
P = pressure
R,R_c = radius and throat radius of curvature (Fig. 2)
r,z = radial and axial coordinates (Fig. 1)
$r_{\min}$ = throat radius (Fig. 1)
u,w = radial and axial velocity components (Fig. 1)
V = total velocity
α,θ = divergent and convergent cone half-angles (Fig. 2)
γ = specific heat ratio
ρ = density

Subscripts

i = strip boundary
j = number of strips
k = counter between 0 and j, see Eqs. (17) and (18)

Introduction

THE survey papers of Hall and Sutton,[1] and of Sichel[2] outline progress with theories for nozzle flow, the latter paper in the wider context of viscous transonic flow. Other newer techniques are those of Moretti adapted by Midgal et al.,[23] and of Thompson.[22] Recently Alikhaskin et al.,[3,4] Van Zhu Tsuan,[4] Belotserkovskii and Chushkin[4] and Holt[5] have introduced to the nozzle problem the method of integral relations (MIR),[6] which had been successful in solving other transonic flow problems,[4] notably the supersonic blunt body.[7,8] The solutions of Refs. 3 and 5 are indirect and of first order (one strip). The others are direct solutions for given shapes of two-dimensional, axisymmetric and annular nozzles. The published solutions are, however, for restricted shape families. This paper sets out to solve the direct problem for arbitrarily shaped nozzles, in particular those commonly found in use for rockets. Attention is concentrated on conical axisymmetric nozzles. The gas is taken as perfect and inviscid, and all results are for $\gamma = 1.4$. Simple cylindrical coordinates are chosen (Fig. 1).

It is emphasized that although more accurate techniques such as the method of characteristics are available for the supersonic flow, an attempt was made to obtain the complete subsonic, transonic and supersonic flowfield with the one method without the need for patching.

In the more restricted range of incompressible flow the method has also been applied by the present authors.[25]

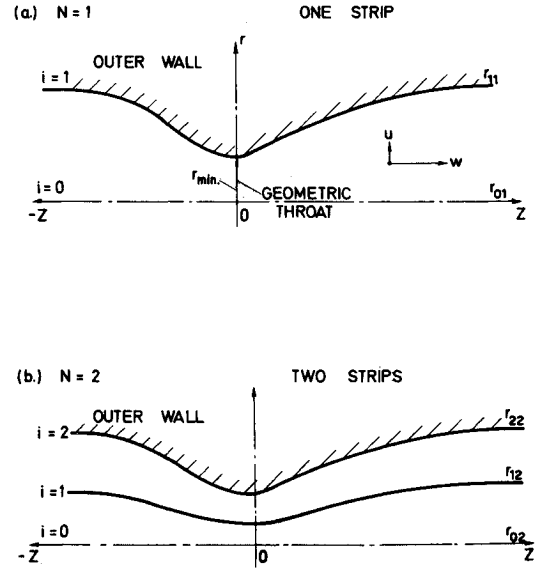

Fig. 1 Designation of strips.

Received September 8, 1970; revision received February 25, 1971.

* Senior Research Engineer, Emissions Research Department. Member AIAA.

† Senior Lecturer, School of Mechanical and Industrial Engineering, on leave at Department of Aeronautics, Imperial College, London, England. Member AIAA.

‡ All lengths are rendered dimensionless by reference to $r_{\min}$.

Method of Integral Relations Applied to the Direct Nozzle Problem

Belotserkovskii's treatment[7,8] of the supersonic blunt body used the continuity and transverse momentum equations of the shock layer transonic field in two independent space variables. He recast the two nonlinear partial differential equations as simultaneous ordinary differential equations by using "integral relation" approximations during integration on one of the independent variables. The second integration could then be mechanized using standard numerical procedures.

Following experience with this method,[9] the same approach was tried here. However, the statement of the problem was found to be less complex if the two partial differential equations chosen to describe the transonic field were the continuity and irrotationality relations. Since homentropic flow was assumed, the restriction of shock-free flow applies.

The equations of motion in normalized variables are taken as:

Continuity

$$\partial/\partial r\ (\rho u r^n) + \partial/\partial z\ (\rho w r^n) = 0 \tag{1}$$

Irrotationality

$$\partial w/\partial r - \partial u/\partial z = 0 \tag{2}$$

Entropy

$$P = \rho^\gamma \tag{3}$$

Integrated momentum

$$\rho = \{1 - [(\gamma - 1)/(\gamma + 1)]V^2\}^{1/(\gamma-1)} \tag{4}$$

The pressure and density are normalized by referring to stagnation values, and velocity is normalized by referring to the corresponding maximum possible velocity. The reference length is the throat radius, $r_{\min}$, (Fig. 1). Equation (4) is obtained by integrating the momentum equation and using Eq. (3).

Boundary conditions on velocity are, at the wall:

$$u_{jj} = w_{jj}(dr_{jj}/dz) \tag{5}$$

and on the axis:

$$u_{0j} = 0 \tag{6}$$

Initial conditions on the upstream plane face at inlet are found by iteration, and downstream boundary values are set by conditions at the throat. Equations (1) and (2) are in the desired "divergence" form of the MIR.[6]

To illustrate the use of the method here, we will apply it to the irrotationality equation. (The full treatment of the continuity equations and the irrotationality equation for the general case can be found in Ref. 10). The flowfield is divided into N strips. Figure (1a) shows one strip ($N = 1$), and Fig. (1b) two strips ($N = 2$). Our example will use the one-strip solution. Equations (1) and (2), when integrated across the strips in the r direction, will yield ordinary differential equations if remaining integrands are approximated. These approximations are called the "integral relations" and use the values of the integrands at the strip boundaries. As a result, the order of the approximation will depend on the number of strips. In a simple one-strip solution, the approximation employs only center-line and wall values of the integrand. Integrating the irrotationality equation from the centerline, $r = 0$, to the wall, $r = r_{11}$:

$$w_{11} - w_{01} - \int_0^{r_{11}} \frac{\partial u}{\partial z}\, dr = 0 \tag{7}$$

Apply Liebnitz's Rule and the inner wall boundary condition:

$$w_{11} - w_{01} - \frac{d}{dz}\int_0^{r_{11}} u\,dr + u_{11}\frac{dr_{11}}{dz} = 0 \tag{8}$$

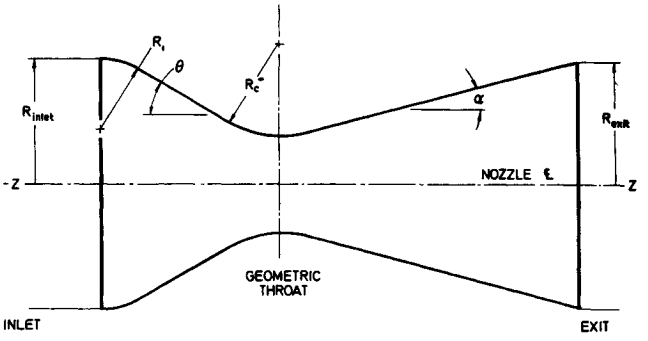

Fig. 2 Conical nozzle geometry.

An approximation must now be made for the integrand u. It is presumed to be a continuous and bounded function of r/r_{jj}, and must by symmetry be an odd function. Thus, there exists a real polynomial approximation for u:

$$u = \sum_{k=1}^{j} [u]_k \left(\frac{r}{r_{jj}}\right)^{(2k-1)} \tag{9}$$

where the $[u]_k$ terms are functions of u at the strip boundaries. For $N = 1$,

$$u = [u]_1 r/r_{11} \tag{10}$$

When $r = r_{11}$, then $[u]_1 = u_{11}$, and

$$u = u_{11} r/r_{11} \tag{11}$$

Equation (11) can now be integrated between the limits of $r = 0$ and $r = r_{11}$,

$$\int_0^{r_{11}} u\,dr = \frac{u_{11} r_{11}}{2} \tag{12}$$

Substituting Eq. (12) into Eq. (8) transforms it into an ordinary differential equation:

$$w_{11} - w_{01} - \tfrac{1}{2}(d/dz)(u_{11} r_{11}) + u_{11}(dr_{11}/dz) = 0 \tag{13}$$

Use the outer wall boundary condition, and rearrange in a form suitable for numerical integration:

$$dw_{11}/dz = [2w_{11} - 2w_{01} - w_{11} r_{11}(d^2 r_{11}/dz^2) + w_{11}(dr_{11}/dz)^2]/[r_{11}(dr_{11}/dz)] \tag{14}$$

Since the shape of the wall is specified, r_{11} and its derivatives are known. The only unknowns are w_{01} and w_{11}, the axial components of velocity at centerline and wall.

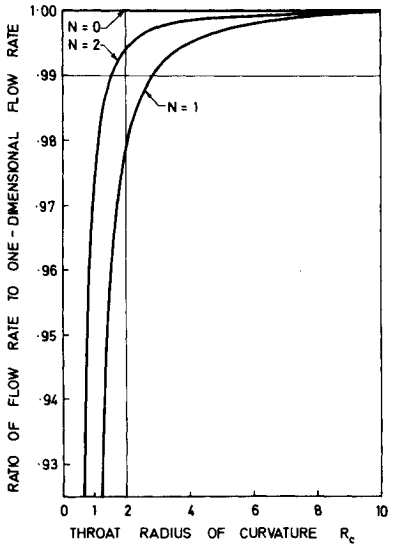

Fig. 3 Flow rates.

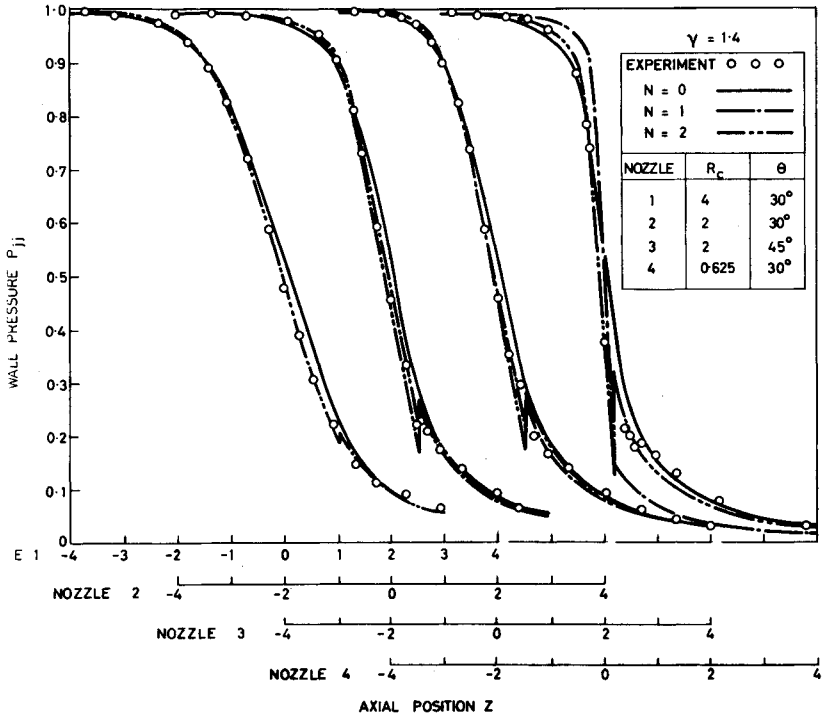

Fig. 4 Wall pressure, nozzles 1–4.

Similar treatment of Eq. (1) produces an expression for dw_{01}/dz, [Eq. (A2)]. The integrand to be approximated in this case is ρw. Symmetry dictates that it be an even function, and, therefore:

$$\rho w = \sum_{k=0}^{j} [\rho w]_k \left(\frac{r}{r_{jj}}\right)^{2k} \tag{15}$$

When $N = 1$, the first two terms of the polynomial are used. Evaluating the equations at $r = 0$ and at $r = r_{11}$ yields expressions for $[\rho w]_0$ and $[\rho w]_1$. When these are substituted back into Eq. (15), the result is:

$$\rho w = \rho_{01} w_{01} + (\rho_{11} w_{11} - \rho_{01} w_{01})(r/r_{11})^2 \tag{16}$$

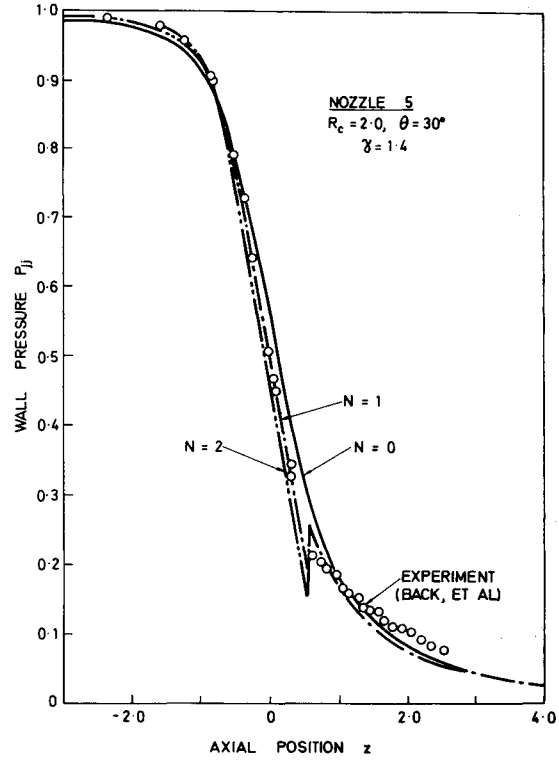

Fig. 5 Wall pressure, nozzle 5.

This enables Eq. (1) to be integrated from $r = 0$ to $r = r_{11}$. Equations (3) and (4), written for both the centerline and the wall, complete the system of equations for one strip (Appendix A).

The equations for dw_{11}/dz and dw_{01}/dz are now simultaneous ordinary differential equations, which can be integrated by standard numerical methods. The method will yield the familiar one-dimensional equations, by taking $N = 0$ and placing $j = 0$ in Eqs. (9) and (15). Thus, u is zero and ρw no longer depends on r. The accuracy of the solution can be increased by using a larger number of strips and hence a larger number of terms in approximating polynomials. For the irrotationality equation, the number of terms in the polynomial of Eq. (9) is the same as the number of strips, N. For the continuity equation, the number of terms in Eq. (15) will be $N + 1$.

The scheme chosen to divide the field into strips was to select equal intervals in r. Thus, when the flowfield is divided into two strips ($N = 2$) the additional strip boundary is located at $r_{12} = r_{22}/2$ (Fig. 1b). The continuity and irrotationality equations are first integrated from $r = 0$ to $r = r_{12}$, and then from $r = 0$ to $r = r_{22}$. The resulting four simultaneous differential equations can then be integrated numerically. To solve for all of the variables, the momentum and entropy equations must be written on the three boundaries: centerline, intermediate line and wall. For annular and asymmetric plane nozzles, the lower limit of integration will be $r = r_{0j}$ rather than $r = 0$. The system of equations in two strips is given in Appendix B.

In general, when integrating the continuity equation, for any number of strips $j = N$, the approximation, or "integral relation" required is:

$$\int_{r_{oi}}^{r_{ij}} f r^n dr = \frac{(r_{jj} - r_{0j})^{n+1}}{a_{ij}} \sum_{k=0}^{j} b_{kij} f_{kj} \tag{17}$$

where f is ρw. The approximation required in the irrotationality equation is:

$$\int_{r_{oi}}^{r_{ij}} u dr = \frac{r_{jj} - r_{0j}}{a_{ij}} \sum_{k=0}^{j} b_{kij} u_{kj} \tag{18}$$

a_{ij} and b_{kij} are numerical coefficients which, together with f_{kj} and u_{kj}, are listed in Ref. 10 for $N = 0$–3. Equations (17)

Table 1 Conical nozzles, $\alpha = 15°$ (Fig. 2)

Nozzle No.	R_{inlet}	R_c	R_I	θ	Expt.	r_{min} (in.)	R_{exit}
1	2.684	4.000	1.500	30°	Ref. 10	0.750	2.684
2	2.684	2.000	1.500	30°	Ref. 10	0.750	2.684
3	2.684	2.000	1.500	45°	Ref. 10	0.750	2.684
4	2.684	0.625	1.500	30°	Ref. 10	0.750	2.684
5	2.810	2.000	1.575	30°	Ref. 20	0.902	1.630
6	3.125	0.625	1.000	45°	Ref. 16	0.800	2.572
7	3.00	2.00	12.00	30°	...	...	...
8	3.00	2.00	0.75	75°	...	...	...
9	3.00	10.00	3.00	30°	...	...	...
Smooth	3.00	4.00	3.00	30°	...	...	...

and (18) not only allow for incompressible ($f = w$) and compressible flow ($f = \rho w$), plane ($n = 0$) and axisymmetric flow ($n = 1$), but also asymmetric, plane and annular axisymmetric flow ($r_{0j} \neq 0$).

Numerical Computation

The equations for $N = 1$ and 2 are presented in a form ready for use in computation in Appendices A and B. The Runge-Kutta numerical integration procedure was used most often here.

To start the integration, initial conditions must be specified. In the one strip case, this can be done by noting that at the entrance and at the throat of the nozzle, the slope of the wall is zero ($dr_{11}/dz = 0$). At these locations, the denominator of Eq. (A1) is zero. Since dw_{11}/dz must be finite,

$$2w_{11} - 2w_{01} - w_{11}r_{11}(d^2r_{11}/dz^2) = 0 \tag{19}$$

This equation can be rewritten as

$$w_{01}/w_{11} = 1 - \tfrac{1}{2}r_{11}(d^2r_{11}/dz^2) \tag{20}$$

At the throat of the nozzle, d^2r_{11}/dz^2 must be either zero or a positive finite quantity. As a result, the wall velocity, w_{11}, will always be equal to or larger than the centerline velocity, w_{01}. When the wall curvature is zero, $d^2r_{11}/dz^2 = 0$, and the flow is uniform ($w_{01} = w_{11}$).

The continuity equation (A2) can be integrated analytically at any station to yield the mass flow

$$[(8 - 5n)\rho_{01}w_{01} + (4 - n)\rho_{11}w_{11}]r_{11}^{(n+1)} = F \tag{21}$$

If Eqs. (20) and (21) are applied at the throat for an assumed value of w_{11}, the flow rate F can be calculated. The same equations can then be applied at the entrance, together with the value of the flow rate F just found, to determine the required initial values of w_{01} and w_{11} to commence the integration. If the flow is subsonic, each value of w_{11} corresponds to a particular value of flow rate F. In the case of supersonic flow, the flow rate is a maximum. The value of w_{11} at the throat corresponding to this maximum flow rate is found by substituting Eq. (20) into Eq. (21), and differentiating with respect to w_{11}, then setting the derivative $dF/dw_{11} = 0$ and solving for w_{11} with the help of Eqs. (A3) and (A4). Having obtained w_{11}, w_{01} is computed from Eq. (20) and the flow rate F from Eq. (21). Using the flow rate F, the initial conditions at the nozzle entrance are computed as before.

In the two-strip case, there are four unknown initial values: radial velocity u_{12}, and axial velocity components w_{02}, w_{12} and w_{22}. Two of the four, w_{02} and w_{22}, may be removed by two conditions similar to those for one strip. Thus, for continuity of the solution at a singularity, use Eq. (B1) instead of Eq. (A1), and for the flow rate F the integrated continuity equation (B-10). The flow rate, however, must be assumed as well as the initial values of u_{12} and w_{12}. If the initial values of u_{12} or w_{12} are in error, w_{02} or w_{22} will go to zero during the course of the integration. Iteration proceeds until the solution can be carried up to the throat. If the computed and assumed flow rates disagree there, it is necessary to select a new flow rate and begin again.

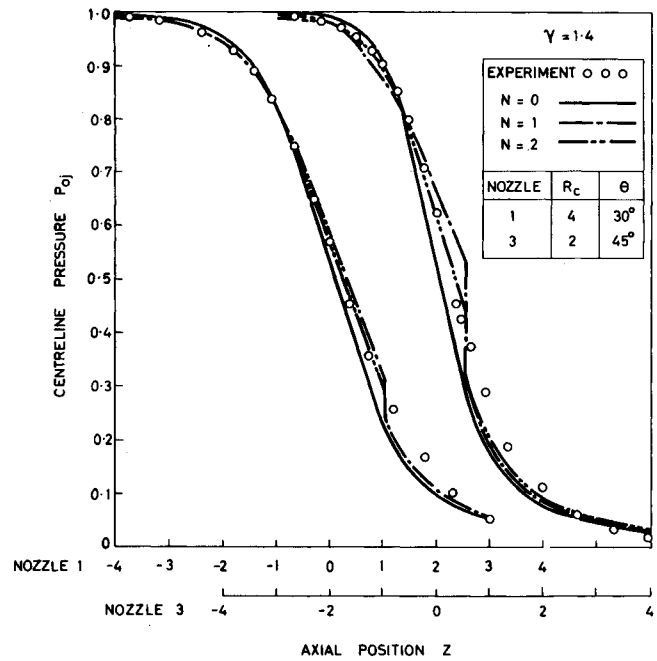

Fig. 6 Centerline pressure, nozzles 1 and 3.

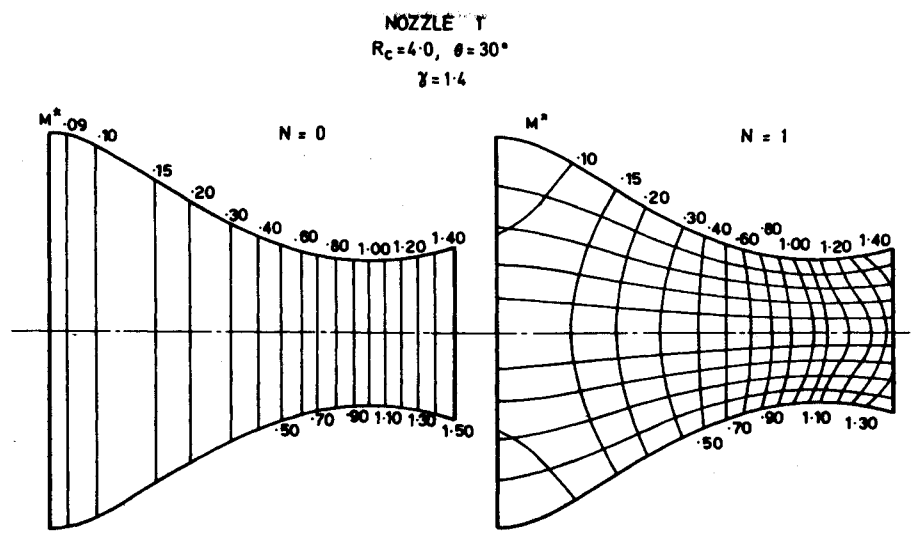

Fig. 7 Velocity field, nozzle 1; $N = 0,1$.

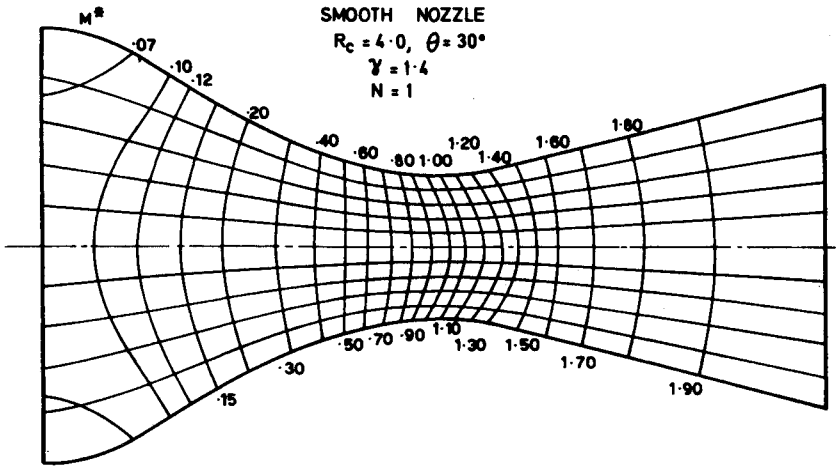

Fig. 8 Velocity field, smooth nozzle; $N = 1$.

Solutions for three or more strips present many additional difficulties in the numerical analysis.[10]

When the nozzle profile has curvature discontinuities, such as those which occur at tangent points on the wall of a conical nozzle (Fig. 2), velocity discontinuities arise in the solution. These are too small to appear in the subsonic contraction. Integration in such a region was found to be stable by reducing step size. The geometric throat singularity also required a smaller step size locally and in addition a scheme to extrapolate across the singularity itself.

Integration was always possible beyond the geometric throat up to and across the axial sonic points. Downstream of this, however, the integration soon became unstable, no matter how refined the solution. Stability returned if the direction of integration was reversed, that is, by jumping to the nozzle exit plane, and integrating back towards the sonic line. This process required iteration on assumed "initial" velocities at the exit plane. A first guess was obtained by assuming the flow to be a conic point source flow. Applying the integrated continuity equation, Eq. (A7) or Eq. (B10) and the known flow rate, the integration and iteration proceeded until a match was obtained at the sonic line.

A basic nondimensional step size of 0.005 was found to give reasonable computing time for accuracy to seven significant figures and stability in z to 0.10. Computing time on an IBM 360 model 50 for the one strip case was about 75 sec for a single run covering both the convergent and divergent sections. A two-strip solution required 2 min per iteration on either the convergent or the divergent sections, and about twenty iterations to converge to a satisfactory solution.

All numerical results are for $\gamma = 1.4$. The calculated flow rate through the conical nozzles is shown in Fig. 3 as a fraction of the one-dimensional flow rate for a range of throat radius of curvature and for $N = 1$ and 2. Wall static pressure distributions (Figs. 4 and 5), and centerline pressures (Fig. 6) are for the conical nozzles 1–5, Table 1. Typical velocity fields are shown in Figs. 7 and 8. The "smooth" conic nozzle uses higher order polynomials at tangent points to conic walls in order to avoid curvature discontinuity there.

Experiment

Four nozzles, with the profiles described by nozzles 1–4 in Table 1, were tested with air at ambient stagnation temperature, in the School of Mechanical and Industrial Engineering at the University of New South Wales. The air was supplied at pressures up to 125 psia by two 150-hp compressors, and stored in a 1000-ft^3 reservoir. The rated capacity of both compressors is 1.5 lb/sec at 135 psia. Alumina dessicant was used to dry the air to $-50°$F dewpoint.

A manual 4-in. gate valve was used to control stagnation pressure. A screen box and settling chamber were included to reduce turbulence. During wall pressure tests, a 64-in. length of 4-in. pipe, bolted to the nozzle exit, acted as a diffuser. With this fitted, exit velocities up to Mach 3.5 were achieved. For tests to determine centerline pressure, a pressure probe housing was bolted between the nozzle and the diffuser.

Wall static pressures were measured at 22 points along the profile. The pressure taps were 0.032 in. in diameter and drilled normal to the wall. Static pressures were read by twelve 6-in. Bourdon tube gauges, which calibrations showed to be consistently accurate to 0.5%. Data were recorded by photographing all gages simultaneously.

The centerline pressure probe for supersonic flow was an open-ended, 1-mm-diam tube and measured the stagnation pressure behind the normal shock in front of the probe. The static pressure immediately upstream of the shock was determined using the measured stagnation pressures across the normal shock. The shock stand-off distance was determined from Ref. 11. In subsonic flow, a slotted static pressure probe was chosen. The slots, located 15 diam back from the nose, improved response by providing a larger area than drilled holes. The pressure error is estimated to be no more than 0.2%.[12] The estimated over-all error of the data, including instrument and reading error, is 1.5%, and is consistent with the observed data scatter.

During the course of the supersonic centerline pressure distribution tests, oblique shocks were observed. The existence of oblique shocks in conical nozzles has been predicted by Migdal and Landis,[13] Migdal and Kossen,[15] and Darwell and Badham,[14] and a shock was observed in such a nozzle (nozzle 6 of Table 1) with a throat radius of curvature of 0.625 by Back and Cuffel.[16] In the work carried out here, shocks were observed in all four of the nozzles tested. The shock angle (from the centerline of the nozzle) varied with the throat radius of curvature R_c, from 6.7° for nozzle 1 with $R_c = 4$, to 14° for $R_c = 2$ (nozzles 2 and 3), and to 18° for $R_c = 0.625$ (nozzle 4). In all cases, the shock appeared to originate at the tangent point between the circular arc throat and the exhaust cone. The numerical results (Figs. 4 and 5) predict a wall pressure rise at this point which in supersonic flow can be consistent with a shock. The presence of a shock wave in the exhaust cones of a conical nozzle will invalidate the theoretical method of this paper there.

Discussion

In the subsonic and transonic flow ahead of the shock, wall pressures (Fig. 4) are well predicted by the one-strip solution for throat radii of curvature R_c greater than 2. But centerline pressures (Fig. 6) required the two-strip solution, although the trend indicates that a two-strip solution is not necessary for $R_c > 4$. The two-strip solutions for centerline pressures lie between the one-dimensional and one-strip solu-

tions. The flow rate calculations (Fig. 3) show the same behavior over the whole range of R_c, the one-strip solution yielding a value too low and the one-dimensional theory a value too high compared to the two-strip solution. The deviation is less than 1% in each case for $R_c > 2$.

The method of this paper can be compared in Fig. 5 with the experiments of Back et al.[20] on nozzle 5 in Table 1, and with theories of Sauer,[17] Oswatitch[18] and Hall[19] using Fig. 1 of Ref. 20 for the same nozzle, which has $R_c = 2$ and similar geometry to nozzle 2, although 80% larger in scale. The agreement between MIR solutions and experiment is good for both nozzle 2 (tests reported here) and nozzle 5 (tests of Ref. 20), and extends over the entire subsonic and transonic range up to the shock wave. In this respect the MIR has improved on the preceding theories.

The velocity fields for the simple conical nozzle 1 of Fig. 7 are cut off at the divergent wall curvature discontinuity because experiments on nozzles 1–6 showed that each generated a shock wave at that position. However, the strength of the wall pressure change there decreases with increasing throat radius of curvature. The one-strip predictions for nozzles 7–9 reflect the influence on the flowfields of large changes in converging cone angle, inlet and throat radii of curvature. Of these three, only the latter appears to be significant to the flowfield in the throat.

Transverse propagation of the effect of the wall discontinuity into the flowfield, as shown in the solutions for centerline pressure for example (Fig. 6), betrays the dependence of the MIR at such a discontinuity on the selection of the coordinate system, in this case, cylindrical coordinates. Similar comments can be made about the use of the MIR in the supersonic blunt body problem.[21] Nevertheless, the solutions do predict conditions favoring formation both of shocks and the resulting boundary-layer interaction which can be assumed will smooth out the shock pressure discontinuity at the wall. In the most extreme case examined here $R_c = 0.625$ and $\theta = 30°$, the $N = 2$ strip solution gave the best solution upstream of the jump. Unfortunately a direct comparison cannot be made between the MIR solutions given here and a Moretti solution by Migdal et al.[23] who used the experiments of Back et al.[20] on the nozzle $R_c = 0.625$ and $\theta = 45°$. Nor is any direct comparison possible here with the work of Kleigel[24] for high curvature flows.

Smoothing of curvature discontinuity by fitting a higher order polynomial at such a point removes the local velocity field discontinuity of the MIR, although this does not necessarily remove the cause of shock waves in the divergent cone. A complete theoretical flowfield for such a smooth nozzle is shown in Fig. 8 extended into the supersonic divergent cone.

Examples of the use of the method for arbitrarily shaped parabolic and annular nozzles are given in Ref. 10. The latter type of solution opens up the possibility of the application of the method to curved channel flow such as studied by Thompson.[22]

Conclusion

The "method of integral relations" has been applied in cylindrical coordinates to the direct problem of finding the flowfield for given simple conical nozzles. Solutions show good agreement with experiment in the subsonic and transonic regimes ahead of the shock generated at the wall curvature discontinuity at the divergent cone inlet. A one-strip solution is satisfactory for predicting wall pressures in such a nozzle with a throat radius of curvature $R_c \geq 2$ and for predicting centerline pressures when $R_c \geq 4$. A two-strip solution gave good agreement with experimental wall pressures for $R_c \geq 0.625$ and centerline pressures for $R_c \geq 2$. In the presence of shock waves in all nozzles tested, it has not been possible to evaluate the use of the method for isentropic supersonic flow. The method does however predict conditions at the wall favoring the observed shock formation.

Solutions extending into the supersonic regime can be obtained but are not valid unless there are no shock waves or local wall curvature discontinuities.

The numerical method has been used to obtain solutions for other arbitrary shapes including "smooth" conical, parabolic and annular profiles.

Appendix A: $N = 1$ Compressible Flow Equations, Ordinary Nozzles

The differential equations from continuity and irrotationality

$$\frac{dw_{11}}{dz} = \left(\frac{1}{r_{11}\dfrac{dr_{11}}{dz}}\right)\left[2w_{11} - 2w_{01} - w_{11}r_{11}\frac{d^2r_{11}}{dz^2} + w_{11}\left(\frac{dr_{11}}{dz}\right)^2\right] \tag{A1}$$

$$\frac{dw_{01}}{dz} = \left[\frac{\rho_0{}^{(\gamma-1)}}{(8-5n)\rho_{01}(1-w_{01}{}^2)r_{11}}\right]\times \left\{\frac{2(4-n)\rho_{11}w_{11}{}^3r_{11}}{(\gamma+1)\rho_{11}{}^{(\gamma-1)}}\frac{dr_{11}}{dz}\frac{d^2r_{11}}{dz^2} - (n+1)\times [(8-5n)\rho_{01}w_{01} + (4-n)\rho_{11}w_{11}]\,(dr_{11}/dz) - [(4-n)r_{11}\rho_{11}/\rho_{11}{}^{(\gamma-1)}][1 - w_{11}{}^2(dr_{11}/dz)^2 - w_{11}{}^2]dw_{11}/dz\right\} \tag{A2}$$

Momentum

$$\rho_{01} = \{1 - [(\gamma-1)/(\gamma+1)]w_{01}{}^2\}^{1/(\gamma-1)} \tag{A3}$$

$$\rho_{11} = \{1 - [(\gamma-1)/(\gamma+1)]w_{11}{}^2[(dr_{11}/dz)^2 + 1]\}^{1/(\gamma-1)} \tag{A4}$$

Entropy equations

$$P_{01} = \rho_{01}{}^{\gamma}, \qquad P_{11} = \rho_{11}{}^{\gamma} \tag{A5}$$

Boundary conditions

$$u_{11} = w_{11}(dr_{11}/dz), \qquad u_{01} = 0 \tag{A6}$$

Integrated continuity equation

$$[(8-5n)\rho_{01}w_{01} + (4-n)\rho_{11}w_{11}]r_{11}{}^{(n+1)} = F \tag{A7}$$

Appendix B: $N = 2$ Compressible Flow Equations, Ordinary Nozzles

The differential equations from continuity and irrotationality

$$\frac{dw_{22}}{dz} = \left(\frac{1}{3r_{22}\dfrac{dr_{22}}{dz}}\right)\left[14w_{22} - 32w_{12} + 18w_{02} - 16u_{12}\times \frac{dr_{22}}{dz} + 11w_{22}\left(\frac{dr_{22}}{dz}\right)^2 - 3r_{22}w_{22}\frac{d^2r_{22}}{dz^2}\right] \tag{B1}$$

$$\frac{du_{12}}{dz} = \left(\frac{1}{3r_{22}}\right)\left[w_{22} + 8w_{12} - 9w_{02} + u_{12}\frac{dr_{22}}{dz} + w_{22}\times \left(\frac{dr_{22}}{dz}\right)^2\right] \tag{B2}$$

$$\frac{dw_{02}}{dz} = \left[\frac{(n+1)\rho_{02}{}^{(\gamma-1)}}{18\rho_{02}(1-w_{02}{}^2)r_{22}}\right]\left\{-\frac{6\rho_{22}w_{22}{}^3r_{22}}{(\gamma+1)\rho_{22}{}^{(\gamma-1)}}\frac{dr_{22}}{dz}\times \frac{d^2r_{22}}{dz^2} + \frac{3r_{22}\rho_{22}\left\{1 - w_{22}{}^2\left[\left(\dfrac{dr_{22}}{dz}\right)^2 + 1\right]\right\}}{\rho_{22}{}^{(\gamma-1)}}\frac{dw_{22}}{dz} + 64\rho_{12}\times \left(\frac{w_{12}}{2}\frac{dr_{22}}{dz} - u_{12}\right) - \frac{dr_{22}}{dz}[18\rho_{02}w_{02} - 3(n+1)\rho_{22}w_{22}]\right\} \tag{B3}$$

$$\frac{dw_{12}}{dz} = \left\{\frac{1}{12\rho_{12}r_{22}\left[1 - \frac{2w_{12}^2}{(\gamma+1)\rho_{12}^{(\gamma-1)}}\right]}\right\} \times \left[\frac{6r_{22}\rho_{22}w_{22}^3}{(\gamma+1)\rho_{22}^{(\gamma-1)}}\frac{dr_{22}}{dz}\frac{d^2r_{22}}{dz^2} - 8(1-3n)\rho_{12} \times \left(\frac{w_{12}}{2}\frac{dr_{22}}{dz} - u_{12}\right) - (n+1)\frac{dr_{22}}{dz} \times (12\rho_{12}w_{12} + 3\rho_{22}w_{22}) + \frac{24r_{22}\rho_{12}u_{12}w_{12}}{(\gamma+1)\rho_{12}^{(\gamma-1)}}\frac{du_{12}}{dz} - \frac{3r_{22}\rho_{22}\left\{1 - w_{22}^2\left[\left(\frac{dr_{22}}{dz}\right)^2 + 1\right]\right\}}{\rho_{22}^{(\gamma-1)}}\frac{dw_{22}}{dz}\right] \quad \text{(B4)}$$

Momentum

$$\rho_{02} = \{1 - [(\gamma-1)/(\gamma+1)]w_{02}^2\}^{1/(\gamma-1)} \quad \text{(B5)}$$

$$\rho_{12} = \{1 - [(\gamma-1)/(\gamma+1)](u_{12}^2 + w_{12}^2)\}^{1/(\gamma-1)} \quad \text{(B6)}$$

$$\rho_{22} = \{1 - [(\gamma-1)/(\gamma-1)]w_{22}^2[(dr_{22}/dz)^2 + 1]\}^{1/(\gamma-1)} \quad \text{(B7)}$$

Entropy equations

$$P_{02} = \rho_{02}^{\gamma}, \qquad P_{12} = \rho_{12}^{\gamma}, \qquad P_{22} = \rho_{22}^{\gamma} \quad \text{(B8)}$$

Boundary conditions

$$u_{22} = w_{22}(dr_{22}/dz), \qquad u_{02} = 0 \quad \text{(B9)}$$

The integrated continuity equation between centreline and wall is

$$r_{22}^{(n+1)}[(24 - 39n)\rho_{02}w_{02} + (128 - 48n)\rho_{12}w_{12} + (28 - 3n)\rho_{22}w_{22}] = F \quad \text{(B10)}$$

References

[1] Hall, I. M. and Sutton, E. P., "Transonic Flow in Ducts and Nozzles: A Survey," *Transactions of Symposium Transonicum*, Aachen, Sept. 1962, edited by K. Oswatitch, Springer-Verlag, 1964, pp 325–44.

[2] Sichel, M., "Theory of Viscous Transonic Flow—A Survey," *AGARD Conference Proceedings, No. 35, Transonic Aerodynamics*, Paper 10, Sept. 1968.

[3] Alikhashkin, Y. I., Favorskii, A. P., and Chushkin, P. I., "On the Calculation of the Flow in a Plane Laval Nozzle," *Zhurnal Vychislenii Matematiki: Matematicheskoi Fiziki*, Vol. 3, No. 6, June 1963, pp. 1130–4; in English, *Computational Mathematics and Mathematical Physics*, Pergamon Press, May 1967, pp. 1552–8.

[4] Belotserkovskii, O. M. and Chushkin, P. I., "The Numerical Solution of Problems in Gas Dynamics," *Basic Developments in Fluid Dynamics*, Vol. 1, edited by M. Holt, Academic Press, New York, 1965, pp. 1–123.

[5] Holt, M., "The Design of Plane and Axisymmetric Nozzles by the Method of Integral Relations," *Transactions of Symposium Transonicum*, Aachen, Sept. 1962, edited by K. Oswatitch, Springer-Verlag, 1964; also Rept. AFOSR 3140, Sept. 1962, Univ. of Calif., Institute of Engineering Research, Berkeley, Calif.

[6] Dorodnitsyn, A. A., "A Contribution to the Solution of Mixed Problems of Transonic Aerodynamics," *Proceedings of First Congress of Aeronautical Sciences*, Madrid, Sept. 1958, Advances in Aeronautical Sciences, Vol. 2, pp. 832–844.

[7] Belotserkovskii, O. M., "Flow with a Detached Shock Wave about a Symmetric Profile," *Journal of Applied Mathematics and Mechanics*, Vol. 22, 1958, pp. 279–296.

[8] Belotserkovskii, O. M., "Flow Past a Circular Cylinder with a Detacted Shock," *Vych. Mat.* Vol. 3, 1958, pp. 149–185; translation, RAD-9-TM-59-66, Sept. 1959, Avco Corp., Wilmington, Mass.

[9] Archer, R. D. and Herman, R., "Supersonic and Hypersonic Flow of an Ideal Gas around an Elliptic Nose," *AIAA Journal*, Vol. 3, No. 5, May 1965, pp. 987–988.

[10] Liddle, S. G., "A Study of Fluid Flow in Nozzles," Ph.D. thesis, Nov. 1968, Univ. of New South Wales.

[11] Sloan, D., "The Displacement of the Nose Shock Wave from a Pitot Tube under a Streamwise Velocity Gradient," *Journal of the Royal Aeronautical Society*, Vol. 71, Oct. 1967, pp. 725–726.

[12] Pankhurst, R. C. and Holder, D. W., *Wind Tunnel Techniques*, Sir Isaac Pitman and Sons, London, 1952.

[13] Migdal, D. and Landis, F., "Characteristics of Conical Supersonic Nozzles," *ARS Journal*, Vol. 32, Dec. 1962, pp. 1898–1901.

[14] Darwell, H. M. and Badham, H., "Shock Formation in Conic Nozzles," *AIAA Journal*, Vol. 1, No. 8, Aug. 1963, pp. 1932–1934.

[15] Migdal, D. and Kossen, R., "Shock Predictions in Conical Nozzles," *AIAA Journal*, Vol. 3, No. 8, Aug. 1965, pp. 1554–1556.

[16] Back, L. H. and Cuffel, R. F., "Detection of Oblique Shocks in a Conical Nozzle with a Circular Arc Throat," *AIAA Journal*, Vol. 4, No. 12, Dec. 1966, pp. 2219–2221.

[17] Sauer, R., "General Characteristics of the Flow through Nozzles at Near Critical Speeds," TM 1147, 1947, NACA.

[18] Oswatitch, K. and Rothstein, W., "Flow Pattern in a Converging-Diverging Nozzle", TM 1215, 1949, NACA.

[19] Hall, I. M., "Transonic Flow in Two-Dimensional and Axially-Symmetric Nozzles," *Quarterly Journal of Mechanics and Applied Mathematics*, Vol. 15, Pt. 4, Nov. 1962, pp. 487–508.

[20] Back, L. H., Massier, P. F., and Gier, H. L., "Comparison of Measured and Predicted Flows through Conical Supersonic Nozzles, with Emphasis on the Transonic Region," *AIAA Journal*, Vol. 3, No. 9, Sept. 1965, pp. 1606–14.

[21] Kentzer, C. P., "Instability of Numerical Solutions of the Steady, Supersonic Blunt-Body Problem," *AIAA Journal*, Vol. 5, No. 5, May 1967, pp. 1035–7.

[22] Thompson, P. A., "Transonic Flow in Curved Channels," *Transaction of the ASME: Journal of Basic Engineering*, Paper 67-FE-11, Vol. 89, Dec. 1967, pp. 748–752.

[23] Migdal, D., Klein, K., and Moretti, S., "Time-Dependent Calculations for Transonic Nozzle Flow," *AIAA Journal*, Vol. 7, No. 2, Feb. 1969, pp. 372–4.

[24] Kleigel, J. R. and Levine, J. N., "Transonic Flow in Small Throat Radius of Curvature Nozzles," *AIAA Journal*, Vol. 7, No. 7, July 1969, pp. 1375–8.

[25] Liddle, S. G. and Archer, R. D., "Incompressible Flow in Conical Contractions Using the Method of Integral Relations," *Journal of Hydronautics*, Vol. 5, No. 1, Jan. 1971, pp. 25–30.